

THE FAST MULTIPOLE ALGORITHM FOR ANALYSIS OF LARGE-SCALE MICROSTRIP ANTENNA ARRAYS

J. X. Wan, T. M. Xiang, and C. H. Liang

The Department of Electromagnetic Field Engineering
XiDian University
Xi'an, 710071, P. R. China

Abstract—An efficient algorithm combining the fast multipole method (FMM) and the discrete complex image method (DCIM) is presented for analyzing large-scale microstrip structures. Firstly, the effect of complex images' locations on the algorithm is discussed in detail. And a simple and efficient scheme is proposed which greatly enhances the performance of this FMM-DCIM hybrid method. On the other hand, the incomplete LU (ILU) preconditioner with a dual dropping strategy is also tested to study the effect of this preconditioner on the convergence rate of microstrip structures. And experimental results show that this preconditioner reduces the number of iterations substantially. Then the solution is obtained using it in conjunction with the generalized minimal residual (GMRES). The fast multipole method is used to speed up the matrix-vector product in iterations. Numerical results for microstrip antennas are presented to demonstrate the efficiency and accuracy of this method.

1 Introduction

2 Formulations

- 2.1 The FMM with DCIM Solution of the Mixed Potential Integral Equation
- 2.2 Improving the Accuracy of the Closed-form Green's Functions in the Far Field

3 Numerical Results

4 Conclusion

References

1. INTRODUCTION

The method of moments (MoM) has been widely used for the analysis of microstrip structures. However, the numerical solution of the MoM matrix equation requires $O(N^3)$ operations and $O(N^2)$ memory to store the matrix elements, where N is the number of unknowns. The large operation count and memory requirement render the MoM solutions for large-scale problems prohibitively expensive. When an iterative solver is employed for solving the MoM matrix equation, the operation count is $O(N^2)$ per iteration because of the need to evaluate the matrix-vector multiplication. This operation count is too high for an efficient simulation.

To make the iterative method more efficient, it is necessary to speed up the matrix-vector multiplication. There are several techniques developed for this purpose, including the adaptive integral method (AIM) [1], the fast multipole method (FMM) [2, 4], the impedance matrix localization (IML) [5], and the conjugate-gradient fast Fourier transform method (CG-FFT) [6]. Recently, efforts have been made to extend these fast algorithms to microstrip problems. One such example is [7] where the AIM is adapted with the aid of the discrete complex image method (DCIM) [8]. Extension of FMM is difficult because of its dependence on the Green's function. One FMM approach is to express the Green's function in terms of a rapidly converging steepest descent integral and then to evaluate the Hankel function arising in the integrand by FMM [9]. This approach is good for thin-stratified media. The other approach is to combine FMM with DCIM [10–13]. In [10] and [11], which treat the static and two-dimensional (2-D) problems, the equivalent problem is set up by adding images at the corresponding complex coordinates, and therefore, represented by basis functions. In the FMM implementation, the translation is different for different images. In [12], both the 2-D and three-dimensional (3-D) FMM's are employed because the surface-wave poles are extracted in DCIM, which makes the implementation complicated. In [13], the multilevel fast multipole algorithm (MLFMA) [2, 4] combined with DCIM is presented for the efficient analysis of microstrip structures. Instead of being treated separately, the image sources are grouped with the original source. The algorithm requires little extra computation compared with that applied to free space problems.

However, the method in [13] is often affected by complex images' locations. In this paper, the approach of combining FMM and DCIM is discussed in detail. Because of FMM's dependence on the Green's function, the effect of complex images' locations on the efficiency of

FMM is shown firstly. To make the approach of FMM with DCIM applicable, several appropriate complex images must be chosen which may reduce the accuracy of Green's functions in the far field. Or, one must choose the large value of the number of modes L for a high accuracy to be achieved in the far region which degrades the efficiency of FMM. To overcome this problem, a simple and efficient scheme is presented in this paper, which not only makes FMM with DCIM applicable, but also does not increase the complexity of this algorithm. On the other hand, the ILUT preconditioner with a dual dropping strategy is also tested to study the effect of this preconditioner on the convergence rate of microstrip structures. And experimental results show that this preconditioner reduces the number of iterations substantially. Lastly, the solution is obtained using it in conjunction with the generalized minimal residual (GMRES). The fast multipole method is used to speed up the matrix-vector product in iterations. Numerical examples are given to demonstrate the accuracy and efficiency of the method.

2. FORMULATIONS

2.1. The FMM with DCIM Solution of the Mixed Potential Integral Equation

Consider a general microstrip structure residing on an infinite substrate having relative permittivity ϵ_r and thickness h . The microstrip is in the x - y plane and excited by an applied field E^a . The induced current on the microstrip can be found by solving the well-known mixed potential integral equation (MPIE) [14]. First, the microstrip is divided into triangular elements and then the current is expanded using RWG basis functions. Applying the Galerkin's method results in a matrix equation

$$ZI = V \quad (1)$$

in which the impedance matrix has the elements given by

$$Z_{ij} = j\omega \int_{T_i} \int_{T_j} \left[\vec{f}_i(\vec{r}) \cdot G_{Axx}(\vec{r}, \vec{r}') \cdot \vec{f}_j(\vec{r}') - \frac{1}{\omega^2} \nabla \cdot \vec{f}_i(\vec{r}) \nabla \cdot \vec{f}_j(\vec{r}') G_q(\vec{r}, \vec{r}') \right] dr' dr \quad (2)$$

where \vec{f}_i and \vec{f}_j represent the testing and basis functions, respectively, T_i and T_j denote their supports, G_{Axx} is the xx -component of the Green's function for vector potential, and G_q is the Green's function for scalar potential. In general, both G_{Axx} and G_q can be expressed as an

inverse Hankel transform of their spectral domain counterparts, which is commonly known as the Sommerfeld integral (SI). The analytical solution of the SI is generally not available, and the numerical integration is time consuming. This problem can be alleviated using DCIM [8], which yields closed-form expressions as

$$\overline{\overline{G}}_A = \sum_{i=0}^{N_A} a_i^A \frac{e^{-jkR_i^A}}{4\pi R_i^A} \quad (3a)$$

$$G_q = \sum_{i=0}^{N_q} a_i^q \frac{e^{-jkR_i^q}}{4\pi R_i^q} \quad (3b)$$

where $R_i^A = |r - (r' + \hat{z}b_i^A)|$ and $R_i^q = |r - (r' + \hat{z}b_i^q)|$. a_i^A , b_i^A , a_i^q and b_i^q are the complex coefficients obtained from DCIM.

To use FMM, we first divide the entire structure into groups denoted by $G_m (m = 1, 2, \dots, M)$. Letting \vec{r}_i be the field point in a group centered at \vec{r}_m and \vec{r}_j be the source point in a group centered at $\vec{r}_{m'}$, we have

$$\begin{aligned} \vec{r}_{ij} &= \vec{r}_i - (\vec{r}_j + \hat{z}b_i) \\ &= (\vec{r}_i - \vec{r}_m) + (\vec{r}_m - \vec{r}_{m'}) + (\vec{r}_{m'} - \vec{r}_j) - \hat{z}b_i \\ &= \vec{r}_{im} + \vec{r}_{mm'} - \vec{r}_{jm'} - \hat{z}b_i \end{aligned} \quad (4)$$

where $b_i = b_i^A$ or b_i^q .

Employing the addition theorem [3], we can rewrite the Green's function in (3) as

$$G_A(\vec{r}_i, \vec{r}_j) \approx \frac{k}{j16\pi^2} \oint \sum_{i=0}^{N_A} a_i^A e^{j\vec{k} \cdot \hat{z}b_i^A} \times e^{-j\vec{k} \cdot (\vec{r}_{im} - \vec{r}_{jm'})} T(\hat{k} \cdot \hat{r}_{mm'}) d^2\hat{k} \quad (5a)$$

$$G_q(\vec{r}_i, \vec{r}_j) \approx \frac{k}{j16\pi^2} \oint \sum_{i=0}^{N_q} a_i^q e^{j\vec{k} \cdot \hat{z}b_i^q} \times e^{-j\vec{k} \cdot (\vec{r}_{im} - \vec{r}_{jm'})} T(\hat{k} \cdot \hat{r}_{mm'}) d^2\hat{k} \quad (5b)$$

where

$$T(\hat{k} \cdot \hat{r}_{mm'}) = \sum_{l=0}^L (-j)^l (2l+1) h_l^{(2)}(\vec{k} \cdot \vec{r}_{mm'}) P_l(\hat{k} \cdot \hat{r}_{mm'}) \quad (6)$$

Substituting (5) into (2), we obtain

$$\begin{aligned} Z_{ij} &= \frac{\omega k}{16\pi^2} \left[\oint S_A(\hat{k}) U_{im}(\hat{k}) \cdot T(\hat{k}, \hat{r}_{mm'}) U_{jm'}^*(\hat{k}) d^2\hat{k} \right. \\ &\quad \left. - \frac{1}{\omega^2} \oint S_q(\hat{k}) V_{im}(\hat{k}) \cdot T(\hat{k}, \hat{r}_{mm'}) V_{jm'}^*(\hat{k}) d^2\hat{k} \right] \quad (7) \end{aligned}$$

where

$$\begin{aligned}
 U_{im}(\hat{k}) &= \int_{T_i} e^{-j\vec{k}\cdot\vec{r}_{im}} \vec{f}_i(\vec{r}) d\vec{r}, \\
 V_{im}(\hat{k}) &= \int_{T_i} e^{-j\vec{k}\cdot\vec{r}_{im}} \nabla \cdot \vec{f}_i(\vec{r}) d\vec{r} \\
 S_A(\hat{k}) &= \sum_{i=0}^{N_A} a_i^A e^{j\vec{k}\cdot\hat{z}b_i^A} \text{ and } S_q(\hat{k}) = \sum_{i=0}^{N_q} a_i^q e^{j\vec{k}\cdot\hat{z}b_i^q}.
 \end{aligned}$$

When an iterative method is used to solve (1), the matrix-vector multiplication can be performed in such a way that the contributions from nearby groups are calculated directly and the far interactions are calculated using (7).

2.2. Improving the Accuracy of the Closed-form Green’s Functions in the Far Field

As we know, the condition for equation (5) to hold is

$$|\vec{r}_{mm'}| > |\vec{r}_{im} - \vec{r}_{jm'} - \hat{z}b_i| \tag{8}$$

Usually, the depth of the microstrip structures is small, and it is very easy to acquire the smaller value b_i . Hence, the large value b_i can lead to a difficulty in implementing FMM. To illuminate this problem, we consider a microstrip line on a substrate with relative permittivity $\epsilon_r = 2.1$, thickness $h = 1.5748$ mm. The frequency is 9.42 GHz. The line is 1.6 mm wide and 160 mm long and is discretized into triangular elements with edge length 1.6 mm, as shown in Fig. 1. $\max|b_i^q|$ for G_q versus the number of complex images is plotted in Fig. 2. The scalar potential Green’s function G_q is given in Fig. 3. Fig. 4 shows the values of matrix elements calculated by using two different approaches: MoM and FMM. In these two approaches, the vector Green’s function consists of three complex images. However, the scalar potential Green’s function consists of ten complex images in

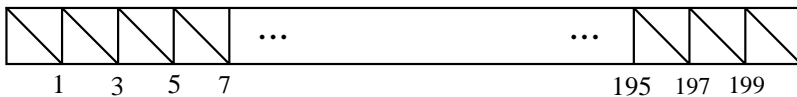


Figure 1. Geometric parameters of a microstrip line $L = 160.0$ mm, $W = 1.6$ mm, the thickness of substrate $h = 1.5748$ mm, $\epsilon_r = 2.1$, $f = 9.42$ GHz.

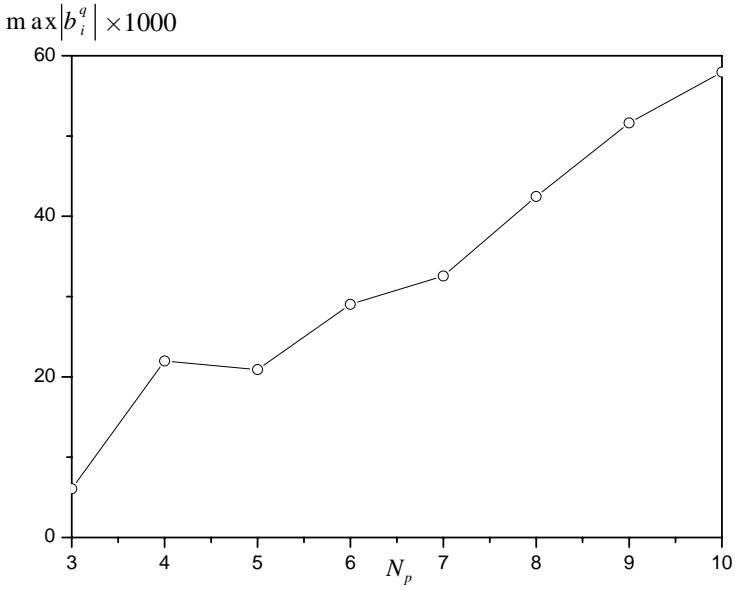


Figure 2. $\max |b_i^q|$ for G_q versus the number of complex images.

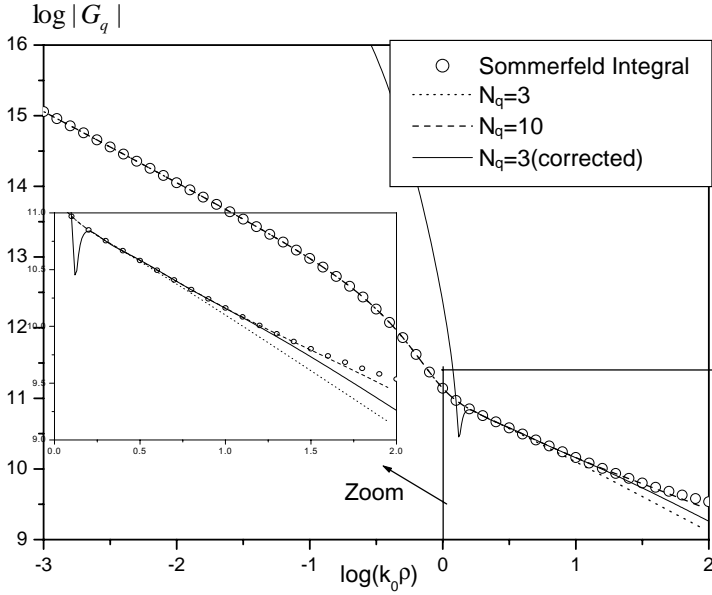


Figure 3. The scalar potential Green's function G_q .

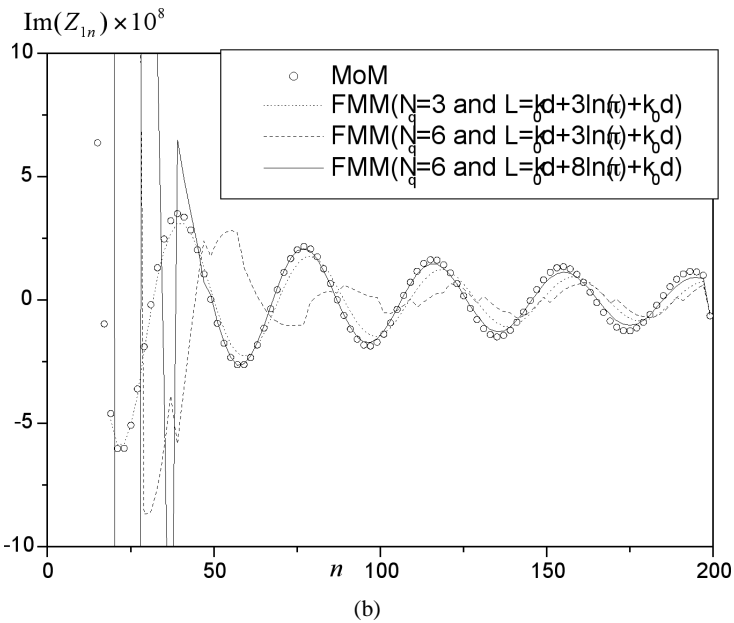
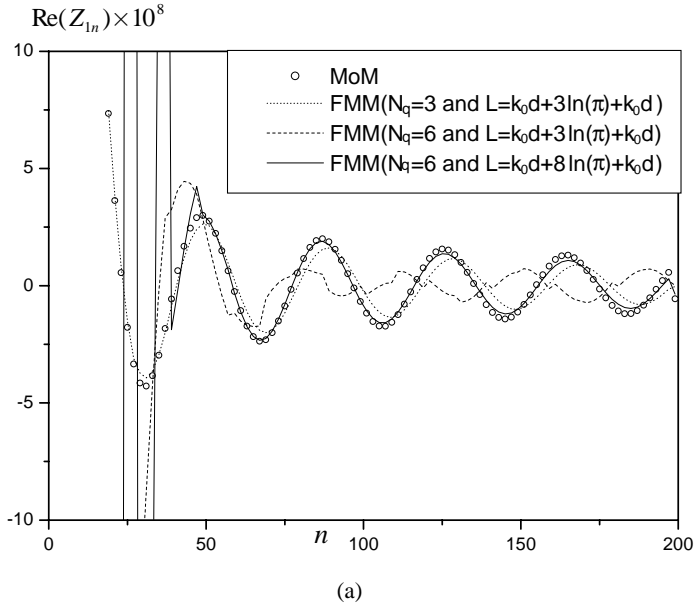


Figure 4. Matrix elements calculated by the conventional MoM and FMM.

MoM. The effect of complex images' locations of the scalar potential Green's function on FMM is studied. The group size d is $0.25\lambda_0$ with λ_0 being the wavelength in free space. Note that $Z_{1n}(n = 1, 3, \dots, 17)$ is considered as the near interaction and is calculated directly, and $Z_{1n}(n = 19, 21, \dots, 199)$ is considered as the far interaction and is calculated by FMM. As seen from Fig. 4, when the number of complex images $N_i^q = 3$ and the number of modes $L = k_0d + 3\ln(\pi + k_0d)$ with k_0 being the wavenumber in free space, the FMM agrees well in the near region, but not in the far region with MoM. The reason is that in this case, $\max|b_i^q|$ is a small enough value and satisfies the condition for (5) to hold. Thus correct results can be obtained in the near region by FMM. But these three complex images and quasi-dynamic images extracted firstly do not give a good approximation of the scalar Green's function G_q in the far field. So it is very difficult to obtain the exact results in the far region. At the same time, we also can see easily that when the number of complex images $N_i^q = 6$ and the number of modes $L = k_0d + 3\ln(\pi + k_0d)$, the FMM does not obtain right results in both the near region and the far region. However, if the number of modes L is chosen to be $k_0d + 8\ln(\pi + k_0d)$, we can find correct solutions in the far region. But in the near region, right results cannot be obtained using FMM because $\max|b_i^q|$ has a large value (as shown in Fig. 2). Furthermore, large values of L correspond to more CPU time requirement that will lead to degraded efficiency of FMM. So, it is desirable to keep L as small as possible. Hence, it is necessary to find a more efficient method to get the solution in the far region instead of using DCIM. It is noted that the source contribution (direct) and its quasi-static image (reflected) contribution can be calculated analytically through Sommerfeld identity. Therefore, they are excluded from complex images in this paper.

It is obvious that the FMM above has a problem: the right results cannot be obtained in both the near region and the far region at the same time. Moreover, one must choose a large value of L for a high accuracy to be achieved in the far region. To overcome this problem, a simple and efficient method is introduced here. Suppose the accurate Green's function is $G_1(\vec{\rho})$, which can be calculated using DCIM or the numerical integral method and so on. The closed-form of the Green's function $G_2(\vec{\rho})$ which is correct in the near region, but may have some slight errors in the far field can be expressed as

$$G_2(\vec{\rho}) = \sum_{p=0}^{N_p} a_p \frac{e^{-jk_r r_p}}{4\pi r_p}, \quad r_p = |\vec{\rho} - \hat{z}b_p|, \quad \vec{\rho} = |\vec{r} - \vec{r}'| \quad (9)$$

where $\max|b_p|$ is with small value. As a rough guideline, we can select $\max|b_p| < 0.6d$ for many applications. $G_2(\vec{\rho})$ can be obtained using

only a few complex images. Now to improve the accuracy of $G_2(\vec{\rho})$ in the far field, we add a correction term

$$G_0(\vec{\rho}) = \sum_{q=1}^{N_q} a_q \frac{e^{-jkr_q}}{4\pi r_q}, \quad r_q = |\vec{\rho} - \hat{z}b_q| \quad (10)$$

where the location of images $b_q (q = 1 \sim N_q)$ are known numbers with small values. The coefficients a_q can be calculated using

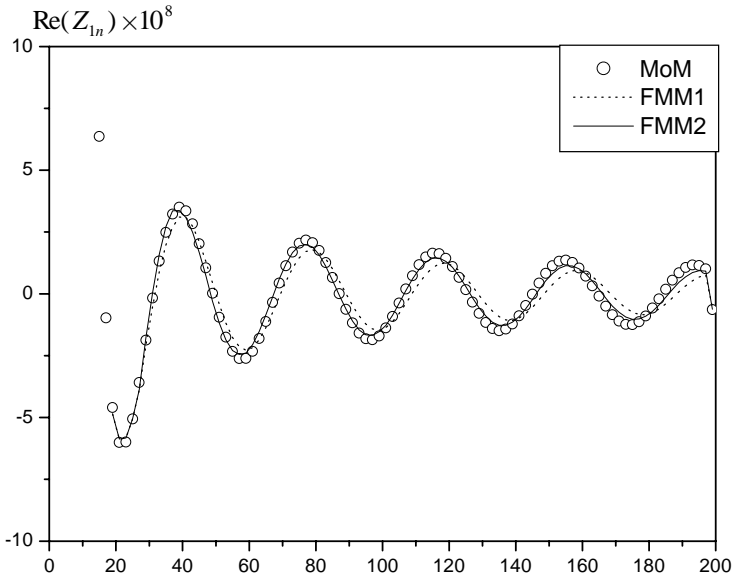
$$G_2(\vec{\rho}) + G_0(\vec{\rho}) = G_1(\vec{\rho}) \quad (11)$$

To find a_q , N_q points $\vec{\rho}$ must be chosen and we need to calculate both sides of (11) at each of these N_q points. Therefore, we will have N_q equations for $a_q (q = 1 \sim N_q)$. Solving these N_q equations with N_q unknowns, we can find a_q . It is noted that sample points should be selected in the far field. To get more accurate results, the least square method is used in this paper. Then the new Green's function in the far field can be given as

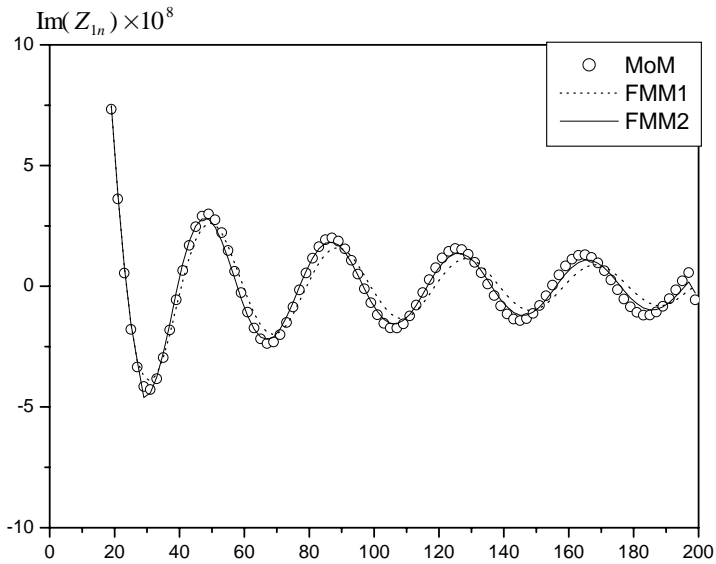
$$G(\vec{\rho}) = G_0(\vec{\rho}) + G_2(\vec{\rho}) = \sum_{q=0}^{N_q} a_q \frac{e^{-jkr_q}}{4\pi r_q} + \sum_{p=0}^{N_p} a_p \frac{e^{-jkr_p}}{4\pi r_p} \quad (12)$$

Now we can implement the FMM. The entire solution region is divided into three regions: near region, mediate region and far region. In the near- and mediate regions, $G_2(\vec{\rho})$ is used. In the far field, $G(\vec{\rho})$ is used, which need computing for only one time. The number of modes L can be chosen to be $k_0d + 3 \ln(\pi + k_0d)$ anywhere. Hence the computational complexity is not increased. Now, our Green's function is correct anywhere. Hence the FMM can be implemented with this closed-form Green's function as it is applied to solve problems in the free space.

To examine the accuracy of this algorithm, a microstrip line shown in Fig. 1 is considered again. Fig. 5 shows the values of matrix elements obtained by using two different approaches. One approach is to use the FMM with three complex images for the scalar potential Green's function, named FMM1. The other approach is to use FMM with the scalar potential Green's function added a correct term in the far region, named FMM2. In this example, we select $N_q = 5$ and $b_q = -0.2 \times q \times h$. In these two FMM, the group size d is $0.25\lambda_0$ with λ_0 being the wavelength in the free space. The number of modes L is chosen to be $k_0d + 3 \ln(\pi + k_0d)$. The Green's function $G(\vec{\rho})$ is plotted in Fig. 3. We can observe that it is more accurate than $G_2(\vec{\rho})$ in the far field. On the other hand, as seen from Fig. 5, the FMM 2 agrees better with MoM. Of course, if we want better results, we must add more terms in $G_0(\vec{\rho})$.



(a)



(b)

Figure 5. Matrix elements calculated by the two different FMM.

3. NUMERICAL RESULTS

The complexity of the fast multipole algorithm has been studied by many authors [3] and is omitted here. In this paper, we study mainly the efficiency of preconditioners and iterative solvers. The iterations are terminated when the relative residual error is less than 10^{-2} . All examples are computed on a Pentium IV 2.4G PC with 512MB of RAM.

In testing microstrip structures, we found that the convergence rate of an iterative solver is very slow. It is well known that the convergence rate of an iterative solution is dependent upon the spectral radius of the MoM system. The reason lies in the large condition number of the system and hence it is imperative to use a preconditioner to offset the slower convergence accruing from the increased spectral radius. The basic principle of preconditioning is to use a matrix to transform the system into an equivalent system so that the spectral radius of the matrix is compressed. A good choice for the matrix should contain most of the dominant terms or the near interactions present in the matrix. In our simulations, the incomplete LU (ILU) preconditioner with a dual dropping strategy is also tested [15] in conjunction with different iterative solvers such as the conjugate gradient normal residual (CGNR) [16], the biconjugate gradient stabilized (BICGSTAB) [17], and the generalized minimal residual (GMRES) [18] to study the effect of this preconditioner and these solvers on the convergence rate of microstrip structures. In the ILUT preconditioner, the dual dropping strategy is implemented using the two parameters τ and p , where τ is the threshold drop tolerance and p is the given-in parameter. Here τ controls the computational cost and p controls the memory cost. By judiciously choosing the two parameters τ and p , we may be able to construct an ILU preconditioner that is effective and does not use much memory space. It should be noted that while CGNR and BICGSTAB require two matrix-vector products for each iteration, GMRES requires only one.

As an example, we consider a four-element series-fed microstrip antenna array, which is fed at the left end. The geometric parameters are taken from [19] and reproduced in Fig. 6. The iteration counts of solvers CGNR, BICGSTAB, and GMRES are tabulated in Table 1 for the ILUT preconditioner and compared to those without using a preconditioner. The maximum number of iterations to allow is 1000.

It is observed that the ILUT preconditioner can effectively bring down the iteration count. It is also observed that both BICGSTAB and GMRES are more efficient than CGNR. Now we select GMRES and study the affect of the different parameters in ILUT on the

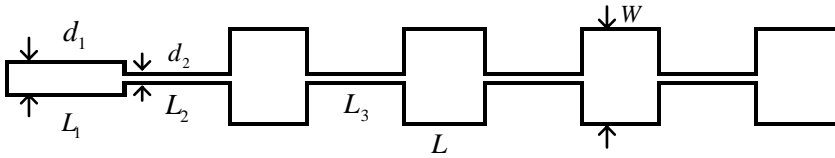


Figure 6. Geometric parameters of a series-fed microstrip antenna array $L = 10.08$ mm, $W = 11.79$ mm, $L_2 = 13.4$, $L_3 = 12.32$, $d_1 = 3.93$ mm, $d_2 = 1.3$ mm, the thickness of substrate $h = 1.5748$ mm, $\epsilon_r = 2.1$, $f = 9.42$ GHz.

Table 1. The iteration counts of solvers CGNR, BICGSTAB, and GMRES for solving radiation by a four-element series-fed microstrip antenna array.

different iterative solvers		CGNR	Bicgstab	Gmres(20)
No Preconditioner	The number of iteration	~	826	~
	The time of solving (1)	~	451.81(s)	~
ILUT(0,0.001)	The number of iteration	64	2	3
	The time of solving (1)	48.01(s)	8.90(s)	8.52(s)

convergence rate. Three cases are tabulated in Table 2. The maximum number of iterations to allow is 200. Obviously, a good quality ILU preconditioners can be obtained by choosing a smaller value of τ and a larger value of p in the ILUT implementation. The E -plane radiation pattern at 9.42 GHz is given in Fig. 7 and is compared with the data given in [20]. Excellent agreement is observed.

Then we consider the plane wave scattering from two finite arrays of microstrip patches of various sizes. The element of the array is a rectangular patch with 36.6 mm width and 26.6 mm length. The distance between two adjacent elements in both the x and y directions is 55.517 mm. The geometry can be obtained from [21]. The monostatic RCS as functions of θ for a 3×3 and 7×7 array at 3.7 GHz are shown in Fig. 8. Good agreement is observed between our results and those obtained by King and Bow [21]. We use GMRES (20) as an iterative solver. The computational requirements of the FMM is listed in Table 3. We can see clearly the efficiency of this fast algorithm.

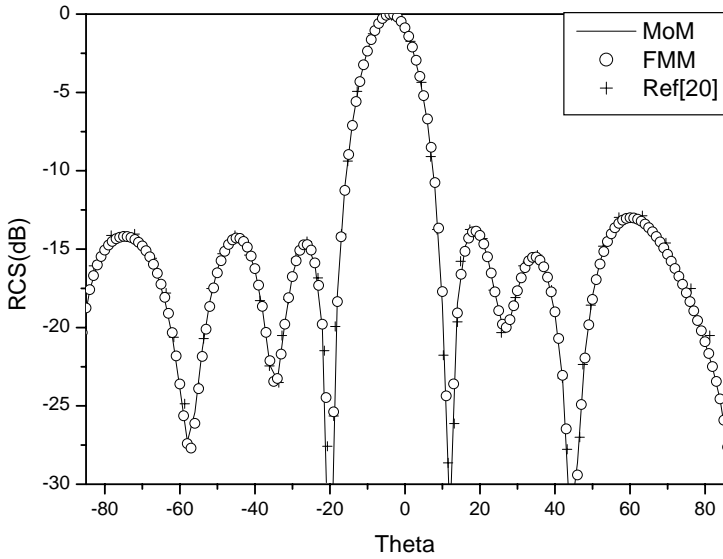


Figure 7. *E*-plane radiation patterns of a series-fed microstrip antenna array.

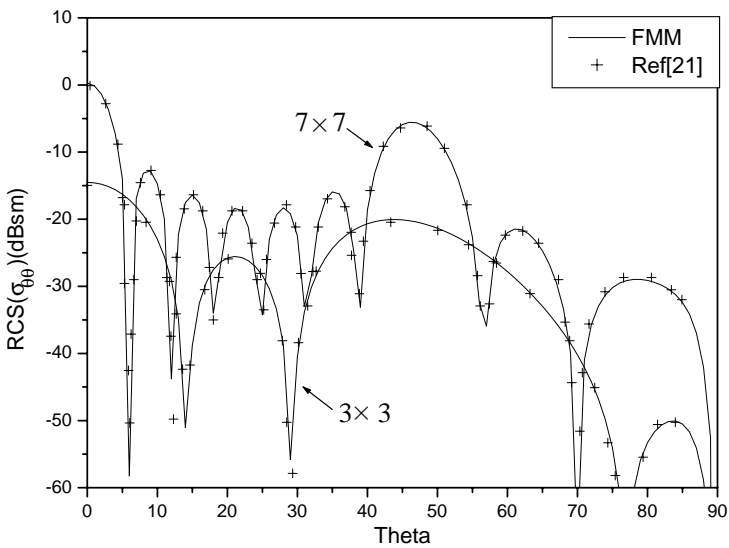


Figure 8. Monostatic RCS ($\theta\theta$) versus θ for various size microstrip patch arrays.

Table 2. The affect of accleration parameters for GMRES (20) for solving radiation by a four-element series-fed microstrip antenna array.

(τ, p)	(0,0.001)	(0,0.01)	(0,0.1)	(20,0.01)	(50,0.01)
The time of make preconditioner (s)	6.92	3.24	~	3.68	4.12
The number of iteration	3	5	~	4	3

In these two tables, symbol "~" means no convergence.

Table 3. Resource requirements of FMM for solving scattering by 3×3 and 7×7 microstrip antenna arrays.

examples	3×3 arrays	7×7 arrays
unknowns	1737	8428
N_{near}	344019	1449616
(τ, p)	(50,0.01)	(50,0.01)
The number of iterative	2	3
The time of make preconditioners (s)	0.66	3.90
The time of each iteration (s)	0.60	7.49

In this table, N_{near} means the number of unknowns solved by MoM.

4. CONCLUSION

In this paper, an efficient algorithm combining the fast multipole method (FMM) and the discrete complex image method (DCIM) is extended successfully to the analysis of scattering and radiation from large-scale microstrip structures. A simple and efficient scheme is presented which makes the approach of the FMM with DCIM applicable. The incomplete LU (ILU) preconditioner with a dual dropping strategy is also tested to study the effect of this preconditioner on the convergence rate of microstrip structures. Numerical results show that the solution can be accelerated using an incomplete LU decomposition preconditioner in conjunction with the generalized minimal residual (GMRES). The fast multipole method

is used to speed up the matrix-vector product in iterations. The FMM also eliminates the need to fill and store the square impedance matrix. Numerical examples demonstrated that the FMM yields a dramatic reduction of memory requirement and computational cost for large problems while retaining good accuracy. Numerical results for microstrip antennas are presented to demonstrate the efficiency and accuracy of this method.

REFERENCES

1. Bleszynski, E., M. Bleszynski, and T. Jaroszewicz, "AIM: adaptive integral method for solving large-scale electromagnetic scattering and radiation problems," *Radio Sci.*, Vol. 31, 1225–1251, Sept./Oct. 1996.
2. Rokhlin, V., "Rapid solution of integral equations of scattering in two dimensions," *J. Comput. Phys.*, Vol. 86, 414–439, Feb. 1990.
3. Coifman, R., V. Rokhlin, and S. Wandzura, "The fast multipole method for the wave equation: A pedestrian prescription," *IEEE Antennas Propagat. Mag.*, Vol. 35, 7–12, June 1993.
4. Song, J. M., C. C. Lu, and W. C. Chew, "Multilevel fast multipole algorithm for electromagnetic scattering by large complex objects," *IEEE Trans. Antennas Propagat.*, Vol. 45, 1488–1493, Oct. 1997.
5. Canning, F. X., "The impedance matrix localization (IML) method for moment-method calculations," *IEEE Antennas Propagat. Mag.*, Vol. 32, 18–30, Oct. 1990.
6. Sarkar, T. K., E. Arvas, and S. M. Rao, "Application of FFT and the conjugate gradient method for the solution of electromagnetic radiation from electrically large and small conducting bodies," *IEEE Trans. Antennas Propagat.*, Vol. 34, 635–640, Oct. 1986.
7. Ling, F., C. F. Wang, and J. M. Jin, "An efficient algorithm for analyzing large-scale microstrip structures using adaptive integral method combined with discrete complex image method," *IEEE APS Int. Symp. Dig.*, Vol. 3, 1778–1781, 1998.
8. Chow, Y. L., J. J. Yang, D. G. Fang, and G. E. Howard, "A closed-form spatial Green's function for the thick microstrip substrate," *IEEE Trans. Microwave Theory Tech.*, Vol. 39, 588–592, Mar. 1991.
9. Zhao, J. S., W. C. Chew, C. C. Lu, E. Michielssen, and J. M. Song, "Thin-stratified medium fast-multipole algorithm for solving microstrip structures," *IEEE Trans. Microwave Theory Tech.*, Vol. 46, 395–403, Apr. 1998.

10. Jandhyala, V., E. Michielssen, and R. Mittra, "Multipole-accelerated capacitance computation for 3-D structures in a stratified dielectric medium using in a closed form Green's function," *Int. J. Microw. Millim.-Wave Comput. Aided Eng.*, Vol. 5, 68–78, May 1995.
11. Gurel, L. and M. I. Aksun, "Electromagnetic scattering solution of conducting strips in layered media using the fast multipole method," *IEEE Microwave Guided Wave Lett.*, Vol. 6, 277–279, Aug. 1996.
12. Macdonald, P. A. and T. Itoh, "Fast simulation of microstrip structures using the fast multipole method," *Int. J. Numer. Modeling: Electron. Networks, Devices, Fields*, Vol. 9, 345–357, 1996.
13. Ling, F., J. Song, and J.-M. Jin, "Multilevel fast multipole algorithm for analysis of large-scale microstrip structures," *IEEE Microwave Guided Wave Lett.*, Vol. 9, 508–510, Dec. 1999.
14. Mosig, J. R., "Arbitrarily shaped microstrip structures and their analysis with a mixed potential integral equation," *IEEE Trans. Microwave Theory Tech.*, Vol. 36, 314–323, Feb. 1988.
15. Saad, Y., "ILUT: a dual threshold incomplete LU factorization," *Numer. Linear Algebra Appl.*, Vol. 1, 387–402, 1994.
16. Greenbaum, A., *Iterative Methods for Solving Linear Systems*, SIAM, Philadelphia, PA, 1997.
17. Van Der Vorst, H. A., "BI-CGSTAB: A fast and smoothly converging variant of BI-CG for the solution of nonsymmetric linear systems," *SIAM J. Sci. Statist. Comput.*, Vol. 13, 631–644, 1992.
18. Saad, Y., "GMRES: A generalized minimal residual algorithm for solving nonsymmetric linear systems," *SIAM J. Sci. Statist. Comput.*, Vol. 7, 856–869, 1986.
19. Wang, C. F., F. Ling, and J. M. Jin, "A fast full-wave analysis of scattering and radiation from large finite arrays of microstrip antennas," *IEEE Trans. Antennas Propagat.*, Vol. 46, 1467–1474, Oct. 1998.
20. Yuan, N., T. S. Yeo, X.-C. Nie, and L.-W. Li, "A fast analysis of scattering and radiation of large microstrip antenna arrays," *IEEE Trans. Antennas Propagat.*, Vol. 51, 2218–226, Sept. 2003.
21. King, A. S. and W. J. Bow, "Scattering from a finite array of microstrip patches," *IEEE Trans. Antennas Propagat.*, Vol. 40, 770–774, July 1992.

Jixiang Wan was born in Henan, China, on May 25, 1978. He received the B.S. and M.S. degrees in electrical engineering from XiDian University, Xi'an, China, in 2000 and 2003, respectively. And he currently is pursuing Ph.D. degree in XiDian University. His research interests include numerical methods for electromagnetic, microstrip antennas, and microwave and millimeter-wave integrated circuits.

Tieming Xiang was born in Jiangsu, China, 1976. He received the B.S. in electrical engineering from XiDian University, Xi'an, China, in 1997. And he currently is pursuing Ph.D. degree in XiDian University. His research interests include numerical methods for electromagnetic and electromagnetic compatibility.

Changhong Liang was born in Shanghai, China, on December 9, 1943. He graduated in 1965 from the former Xidian University, Xi'an, China, and continued his graduate studies until 1967. From 1980 to 1982, he worked at Syracuse University Syracuse, New York, USA as a visiting scholar. He has been a professor and Ph.D. student advisor of Xidian University since 1986. He was awarded the titles "National Middle-Aged and Young Expert with Distinguished Contribution", "National Excellent Teacher", and "One of the 100 National Prominent Professors", etc. Prof. Liang has wide research interests, which include computational microwave and computational electromagnetics, microwave network theory, microwave measurement method and data processing, lossy variational electromagnetics, electromagnetic inverse scattering, electromagnetic compatibility. Prof. Liang is a Fellow of CIE and a Senior Member of IEEE.